Soils and Foundations 2015;55(1):1–16

HOSTED BY

ELSEVIER

The Japanese Geotechnical Society

Soils and Foundations

www.sciencedirect.com
journal homepage: www.elsevier.com/locate/sandf

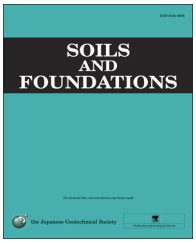

Transitional behaviour in sands with plastic and non-plastic fines

B. Shipton[a,*], M.R. Coop[b]

[a]Arup Geotechnics (formerly Imperial College), Ove Arup and Partners, 13 Fitzroy Street, London W1T 4BQ, UK
[b]City University of Hong Kong, Kowloon Tong, Hong Kong

Received 22 January 2014; received in revised form 24 September 2014; accepted 18 October 2014
Available online 9 January 2015

Abstract

Two model soils, one made from sand with plastic fines and one made from sand with non-plastic fines, were tested in a triaxial apparatus to examine the basic mechanics of transitional soils, that is, soils whose initial density has a very strong influence on the behaviour. The sand with non-plastic fines defined parallel critical state lines and state boundary surfaces at the medium strain levels that can be reached in triaxial testing, the locations of which depended on the initial specific volume of the soil when it was created. Overconsolidating the soil, or shearing it a second time at an increased stress level, was not found to change this behaviour. There was also no significant effect of the initial specific volume on the soil stiffness, which was predominantly a function of the current stress level for normally consolidated states. A variety of different sample preparation methods was used, but the methods did not have any clear influence on the critical state volumes. Although the testing for the sand with non-plastic fines was more limited in extent, the patterns of behaviour seemed to be similar. The relationships between the initial specific volume and the critical state line intercept, Γ, gave gradients of 0.52 and 0.97 for the sands with plastic and non-plastic fines, respectively, showing significant differences in volume remaining after isotropic compression and monotonic compressive shearing.

Keywords: Sands with fines; Triaxial testing; Critical state soil mechanics

1. Introduction

While the behaviour of most soils can generally be described within a critical state framework, there is increasing evidence that there are many soils for which there is a "transitional" mode of behaviour. The term "transitional" refers to the mode of behaviour being intermediate to that of clays and poorly graded sands and has been seen for gap-graded soils (Martins et al., 2001), well-graded clayey silts (Nocilla et al., 2006; Ferreira and Bica, 2006) and well-graded sands (Altuhafi et al., 2010; Altuhafi and Coop, 2011). While several examples of transitional behaviour can now be found, typically for soils of intermediate or mixed grading, it would be incorrect to believe that these constitute the majority of cases, and most soils of intermediate gradings can be described perfectly well within a critical state framework (e.g. Carrera et al., 2011; Vilhar et al., 2013; Duong et al., 2013).

The key features of the behaviour are that compression and shearing are dominated by the initial density of the soil at its creation, so that even compression to high stresses cannot make the compression curves for different initial densities converge onto a unique normal compression line, as a clean sand might do when its behaviour starts to be controlled by particle breakage (e.g., McDowell and Bolton, 1998). Similarly, shearing to modest monotonically applied strains, for example, in a triaxial test, does not give unique critical states in

*Corresponding author.
E-mail address: barbara.shipton@arup.com (B. Shipton).
Peer review under responsibility of The Japanese Geotechnical Society.

http://dx.doi.org/10.1016/j.sandf.2014.12.001

Nomenclature

A	constant in equation $G=Ap'^{n}$
e	void ratio
G	shear modulus
G_s	specific gravity of soil grains
k_0	coefficient of earth pressure at rest
M	gradient of critical state line in q:p' plane
n	exponent in equation $G=Ap'^{n}$
N	projected intercept in v:lnp' plane of isotropic normal compression line at 1 kPa
q	deviatoric stress
p'	mean normal effective stress
p'_{cs}	equivalent pressure taken on the critical state line
p'_e	equivalent pressure taken on the isotropic normal compression line
p'_0	value of p' at start of shearing
SNF	sand with non-plastic fines
SPF	sand with plastic fines
S_{ri}	initial degree of saturation
u	pore pressure
v	specific volume
v_i	initial specific volume
v_{20}	specific volume at $p'=20$ kPa
w_f	final water content
w_i	initial water content
γ_i	initial bulk unit weight
γ_{di}	initial dry unit weight
γ_w	unit weight of water
Γ	projected intercept in v:lnp' plane of critical state line at 1 kPa
ε_a	axial strain
ε_s	shear strain
ε_v	volumetric strain
λ	gradient of critical state line and isotropic normal compression line in v:lnp' plane
σ'_{max}	maximum vertical stress
φ'	angle of shearing resistance
φ'_{cs}	critical state angle of shearing resistance
ψ	state parameter

the v:lnp' plane (v is the specific volume and p' is the mean normal effective stress) that are independent of the initial specific volume (Nocilla et al., 2006; Ferreira and Bica, 2006).

Shipton and Coop (2012) made an extensive investigation of the factors that might give rise to compression behaviour that was not fully convergent, although they recognised that if a single normal compression line could not be identified, this did not necessarily mean that the critical state line would not be unique. They identified non-convergent compression behaviour in a very wide range of soils, both plastic and non-plastic, and observed that particle breakage occurred for the coarse grain component in some of these soils, but not all of them. Two of the soils with the most clearly non-convergent compression behaviour that they identified were simple gap-graded mixtures of sand and either kaolin or crushed quartz fines. This paper presents an investigation of the mechanics of these two soils in shearing, since there is little detailed research on the shearing of transitional soils in the literature. Ferreira and Bica (2006) apparently identified distinct critical state lines for different initial densities for their residual soil. However, the samples were taken from different locations and had slightly different gradings and degrees of weathering. Transitional behaviour was only seen in the remoulded samples, not the intact ones, and also some of their tests were incomplete, perhaps leaving some remaining doubt about their hypothesis of parallel critical state lines. The use of simple constituents also avoids the complex mineralogies of the soils tested by Ferreira and Bica (2006), and so the soils may be easily reproduced by others.

A critical state is a state of constant volume and stress during continued shearing that ideally should also correspond to a unique fabric. The definition was extended by Poorooshasb (1989) to include the condition of a constant lode angle. However, using elongated DEM particles, Nougier-Lehon et al. (2005) found that even for a relatively simple soil, many tens of percent of strain were required to reach a unique fabric, well beyond those that could be applied in simple monotonic element tests, such as triaxial tests. Therefore, many authors have preferred the pragmatic approach, which will be adopted here, of defining critical states as conditions of constant volume and stress reached at the end of triaxial tests, irrespective of whether or not the fabric has been shown to be unique. While this pragmatic approach does of course violate the definition of the critical state, it is not uncommon. Such an approach was used, for example, by Yamamuro and Lade (1998) who observed the clear effects of the initial density on the location of the steady state line in the v:lnp' plane for their silty-sands, which might be described as transitional behaviour, although they did not use this term. Ferreira and Bica (2006) also adopted this approach. For many soils with a natural structure, more stable forms of fabric have been identified; this means that the volumes of the intact soils do not converge with the volumes of the reconstituted soils, even at very large strains (e.g., Coop and Cotecchia, 1995; Fearon and Coop, 2000; Atkinson et al., 2003), and for such soils it has been identified that only vigorous remoulding will break down the fabric. Atkinson et al. (2003) and Fearon and Coop (2000) used a meat grinder to separate the aggregated particles. For soils where such extreme difficulty is found in achieving a unique fabric, the correct definition of a critical state as having a unique fabric begins to seem rather of academic interest as it cannot easily be achieved in practice. In most constitutive models for structured soils, the ultimate volumes of intact and reconstituted soils are assumed to be the same (e.g., Liu and Carter, 2002), but because of the possibility of more stable fabrics, in the framework of Cotecchia and Chandler (2000), implemented as a constitutive model by Baudet and Stallebrass (2004), there is a final difference in the void ratios in

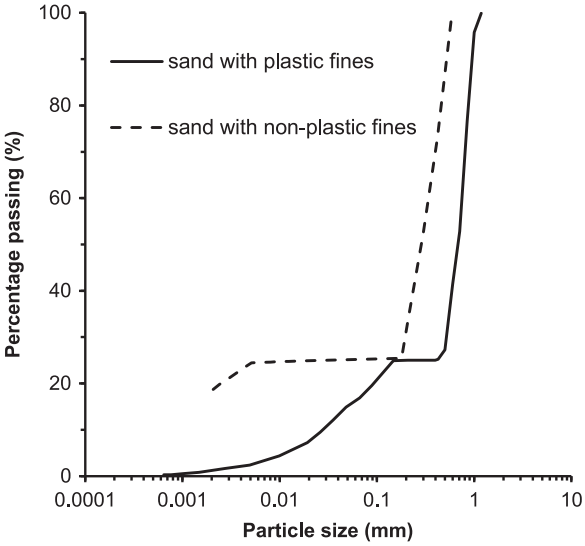

Fig. 1. Particle size distributions.

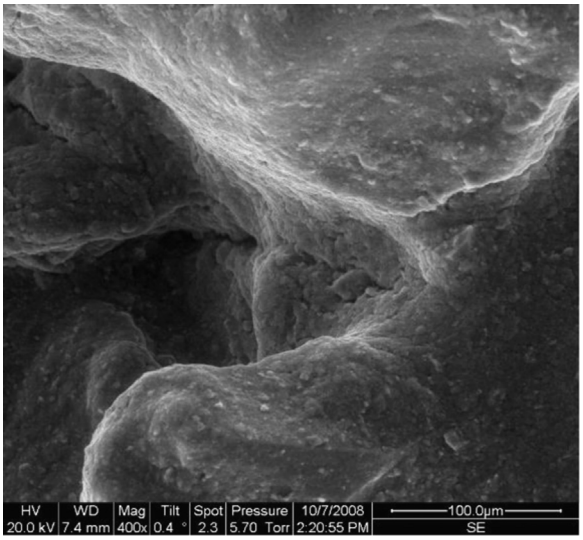

Fig. 2. SEM image of the SPF soil created by compression of slurry in large consolidometer (the image shows a coating of clay particles over sand particles).

compression or at the critical state of the intact and reconstituted soils that no amount of strain will break down.

While the effects of fabric have often been observed to continue to large strains (e.g., Riemer and Seed, 1997; Chen and Chuang, 2001; Chu et al., 2003; Yang et al., 2008), the key feature of transitional soils is the overriding dominance of the initial void ratio, even to the extent that different sample preparation methods that might have been expected to create different fabrics, are less important than the initial density (e.g., Nocilla et al., 2006).

2. Materials tested

The two soils tested were gap-graded mixtures of 75% coarse fraction and 25% fine fraction (Fig. 1), the sand with plastic fines (SPF) having a fines fraction of Speswhite kaolin and the sand with non-plastic fines (SNF) having crushed quartz silt (HPF4, Zdravkovic, 1996). The SPF was made with a sand fraction of Thames Valley sand (Takahashi and Jardine, 2007). Although the constituent soils are from different sources, they are similar to the gap-graded sand–kaolin mixture tested by Martins et al. (2001). Unfortunately, limitations in the supply of this sand meant that a different quartz sand, Redhill sand, had to be used for the SNF. However, the aim of testing the two model soils was to show that similar patterns of transitional behaviour could be seen in sands with plastic and non-plastic fines, rather than to make a detailed comparison of the two soils that are, in any case, artificial.

By using simple constituent particles and gradings, it was also hoped that the fabric might have been quantified. However, the scanning electron microscope image of the SPF in Fig. 2 revealed that there was no feature of fabric that could be easily quantified, the clay particles tending to form a featureless coating over the sand grains no matter what sample preparation technique was used. The larger cavities evident in Fig. 2 may not be macro-voids and more likely simply represent spaces occupied by sand particles pulled out when the broken surface was made. Nocilla et al. (2006) were similarly unable to identify quantifiable elements to explain the transitional behaviour they observed.

2.1. Procedures

Samples were made using a variety of techniques, examining to what extent the behaviour was controlled by the preparation method and to what extent it was controlled by the initial specific volume. The work of Nocilla et al. (2006) and Shipton and Coop (2012) had indicated that the latter was the controlling factor in these soils and that the effects of the sample preparation method were much less important.

For the SPF soil, many of the samples were made from slurries at a variety of water contents by mixing the dry components with deionised water at a variety of water contents. The slurries were then carefully de-aired under a vacuum. Initially, for the triaxial tests, the slurry was loaded to 80 kPa in a 38-mm-diameter floating ring consolidometer, but the disturbance during extrusion led to significant volume changes when the specimens were installed in the triaxial apparatus. The small consolidometer was therefore replaced by a 253-mm-diameter one which made “cakes” through the compression of the slurries to 100 kPa. Sub-samples could then be trimmed with much less disturbance, thus reducing the initial volumetric strains. Carraro and Prezzi (2008) have devised a technique for preparing slurry-based specimens on the triaxial pedestal, avoiding disturbance during trimming. Here, the purpose of the specimen preparation was simply to achieve a range in initial densities rather than a particular target density. One cake was created by the dry compaction of the mixed soil into the consolidometer, after which water was circulated to saturate it before consolidation and sub-sampling for the triaxial testing. Some samples were also created by transferring the slurry directly into the membrane held on the

triaxial pedestal within a split-mould, a negative pore pressure being applied to give the samples sufficient strength to dismantle the mould. Other samples were made by wet compaction of the unsaturated soil into the split-mould, using ten to twelve layers, the undercompaction method being used to ensure uniformity.

The SNF triaxial samples were all made by wet compaction, because when consolidation from slurry was used, the specimen could not retain its suction during trimming and the setting up in the apparatus. However, dry compaction and slurries were also used for the oedometer tests. Details of all the tests performed are given in Tables 1–4.

Table 1
Oedometer test details for the SPF soil (POSXX—slurry sample; POWXX—wet compacted).

Test	v_i	σ'_{vmax} (MPa)
POS01	1.481	14.3
POW02	1.380	28.4
POS03	1.538	8.0
POS04	1.496	8.0
POS05	1.643	8.0

Table 2
Triaxial test details for the SPF soil (D—drained; U—undrained; OC—overconsolidated; Lub. ends—lubricated end platens; v_{20}—initial specific volume at $p'=20$ kPa; p'_0—initial p' for shearing; PSXX—slurry sample; PWXX—wet compacted; PDXX—dry compacted).

Test	v_{20}	p'_0 (kPa)	Shear	Comments
PS00	1.472	600	U	Floating ring consolidometer
PS01	1.418	200	D	–
PS02	1.427	630	U	–
PS03	1.419	200	U	–
PS04	1.453	50	D	–
PS05	1.432	125	D	–
PS06	1.431	70	U	–
PS08	1.477	50	U	–
PS09	1.490	100	D	–
PS10	1.481	400	U	–
PS14	1.442	100	U	–
PS15	1.456	100	D	–
PS16	1.425	500	D	–
PS17	1.461	2300	U	–
PS18	1.443	500	U	–
PS19	1.578	3986	U	–
PD21	1.473	400	D	Dry compacted cake
PD23	1.485	100	U	Dry compacted cake
PW24	1.441	298	D	–
PW25	1.291	698	U	–
PW26	1.325	5000	U	–
PW27	1.316	300	U	–
PS28	1.691	400	U	Created in split-mould
PS29	1.416	400	U	Lub. ends
PD31	1.479	50 ($p'_{max}=5000$)	U	OC, dry compacted cake
PS32	1.506	50 ($p'_{max}=800$)	U	OC, created in split-mould
PW33	1.314	400	D	Lub. ends
PS37	1.444	2300	D	–
PS40	1.572	100/729	D/U	Sheared twice. Created in split-mould
PS41	1.690	100/1000	D/U	Sheared twice. Created in split-mould

Table 3
Oedometer test details for the SNF soil (NOSXX—slurry sample; NOWXX—wet compacted; NODXX—dry compacted).

Test	v_i	σ'_{vmax} (MPa)
NOD01	1.477	7.11
NOS02	1.322	7.13
NOW03	1.600	27.66
NOS04	1.366	13.05
NOD05	1.556	27.63
NOD06	1.304	110.14
NOS07	1.224	110.14
NOW08	1.372	110.14
NOS09	1.272	110.14

Table 4
Triaxial test details for the SNF soil (all wet compacted).

Test	v_{20}	p'_0 (kPa)	Shear
NW01	1.298	700	D
NW03	1.344	200	U
NW04	1.353	200	D
NW06	1.472	–	–
NW07	1.350	333	D
NW08	1.418	1100	U
NW09	1.348	50	D
NW10	1.466	100	D
NW11	1.464	400	D
NW12	1.514	70	D
NW13	1.434	300	U
NW14	1.371	200	U

Triaxial tests were carried out in several computer-controlled hydraulic triaxial apparatuses of standard (800 kPa) cell pressure capacity and one high pressure triaxial apparatus (7 MPa). The former used a platen size of 38 mm and the latter used one of 50 mm, with a 2:1 height: diameter ratio for both. Each had a suction cap to connect the sample top platen to the axial loading system, the connection being made before isotropic compression. Accurate measurements of the axial strains were made either with an LVDT system (Cuccovillo and Coop, 1997) or using inclinometers (Burland and Symes, 1982). In some tests, the radial strains were also measured locally using an LVDT mounted on a belt.

Large strains were required to reach states that were approaching constant stress and volume. Thus, one of the hydraulic triaxial apparatuses was modified so that the axial loading piston had an increased stroke to reach larger axial strains. Lubricated end platens were used in two tests (PW33 and PS29), but in trying to reach the large strains that were desired, problems were encountered with the sample slipping sideways on the platen. Therefore, these were discontinued and most of the tests used conventional platens. As will be discussed later, the effects of end friction in the non-lubricated tests did not significantly influence the data within the context of the very large differences in critical state volumes observed for different initial volumes.

The high pressure apparatus, although stress-path controlled, was a conventional style of triaxial cell, so large axial displacements could be easily applied. Generally, the samples

deformed with only faint signs of localisation. The degree of barrelling in most samples was not severe because the volumetric strains in particular were generally compressive for the SPF samples during shearing. A right cylinder area correction was therefore applied throughout. A correction to the deviator stress was also made for the membrane stiffness, following La Rochelle et al. (1988), but the effect was insignificant at all except the lowest stress levels. In all cases, saturation of the triaxial samples was carried out under back pressure and the B value was ensured to be greater than 95% before the tests were continued.

2.2. Calculation of initial specific volume

In deciding whether a soil has unique normal compression or critical state lines, it is of paramount importance to be able to estimate the accuracy of the specific volumes. Otherwise, it is possible that the inaccuracy of the specific volume measurements might be wrongly interpreted as non-unique lines. Many authors have assessed accuracies from the estimates of the accuracy of individual measurements of weights or dimensions (e.g., Fourie and Papageorgiou, 2001). Fewer have tried to prove the accuracy of their data by comparing different methods of calculation, which is the approach adopted here.

The initial specific volume, v_i, was calculated using Eqs. (1)–(4), chosen to be as independent of each other as possible, although there is some linkage between them.

$$v_i = \left(\frac{w_i G_s}{S_{ri}}\right) + 1 \tag{1}$$

$$v_i = \frac{G_s \gamma_w}{\gamma_{di}} \tag{2}$$

$$v_i = \frac{(G_s - S_{ri})}{(\gamma_i/\gamma_w - S_{ri})} \tag{3}$$

$$v_i = \frac{(w_f G_s + 1)}{(1 - \varepsilon_v)} \tag{4}$$

where w_i and w_f are the initial and final water contents, respectively, γ_{di} is the initial dry unit weight, γ_i is the initial bulk unit weight and ε_v is the overall volumetric strain for the test. Each of these methods uses different measurements made during the tests. Eqs. (1) and (4) are based on the initial and final measurements of the water content, while Eqs. (2) and (3) depend on the dry or saturated weights and the initial dimensions. Ideally all four equations should yield the same value, but each measurement of weight, water content or dimensions will be subject to its own error. Eq. (4) assumes that the sample is saturated at the end of the test. The values of specific gravity G_s were 2.65 for the Redhill sand and the crushed quartz silt, 2.67 for the Thames Valley sand and 2.62 for the kaolin (Martins, 1983; Takahashi and Jardine, 2007; Zdravkovic, 1996).

Due to the multiple methods available for calculating v_i, there is redundancy, and so, there is no need to assume that the soil was initially completely saturated, even for the slurries. For the oedometers, the approach taken was to calculate an average v_i, from Eqs. (2) and (4), assuming saturation at the end of the test in Eq. (4). This value for v_i was then put into Eqs. (1) and (3) to calculate two values for S_{ri}, the mean of which could then be put back into Eqs. (1) and (3) to refine the values for v_i they gave. Not assuming saturation at the start of the test was found to reduce the scatter in v_i. A typical example of the values for v_i, calculated for one test, is given in Table 5. A mean of v_i was taken from the four methods and an estimate of the accuracy made from the maximum deviation of any one value of v_i from the mean, discarding any clearly anomalous data. In this example, the estimated error is ± 0.006, although it should be remembered that the accuracy of the values for G_s dictates that actually the v_i are only valid to 2 dp, the calculations having been made here to 3 dp to avoid rounding errors.

Table 5
Example calculation for the initial specific volume.

Test	v_i equation				Chosen v_i	Estimated accuracy
	1	2	3	4		
PS06	1.499	1.510	1.501	1.505	1.504	± 0.006

Any test with an estimated error of greater than about ± 0.04 for the oedometer tests or ± 0.02 for the triaxial tests was usually discarded. The mean estimated error for the oedometer tests, where all four equations could be used, was about ± 0.01. No consistent bias or greater amount of scatter could be seen in the values from any one of the equations. For the dry compacted samples, only Eq. (2) could be used and an assessment of the accuracy could not be made.

In Table 5, the calculation is made of initial specific volume v_i after saturation in the triaxial cell. As this saturation stage was not at the same p' in each test for all the different preparation techniques, the basis for comparison of specific volumes in Tables 2 and 4, and subsequently in the paper, is the value at p'=20 kPa after saturation and during the initial stages of isotropic compression, v_{20}.

For the triaxial tests, the method of calculation is complicated by the volume change that occurs when the sample is initially set up on the triaxial pedestal and put under back pressure. An overall positive volume change was registered by the volume gauge, but this must have two components; first a positive component from the consolidation of the sample and a second negative component arising from the reduction of air volume in the sample under the back pressure. An iterative procedure was therefore used to estimate the two components. Using the initial degree of saturation, S_{ri}, calculated as above, a correction to the volumetric strain was made assuming that all of the air in the sample was replaced by water. The revised volumetric strain could then be used in Eq. (4) and the calculation repeated until it converged. This method was found to give a mean estimated accuracy of about ± 0.005.

2.3. Compression

Compression data for the two soils are shown in Fig. 3. To compare the oedometer tests with the isotropic compression

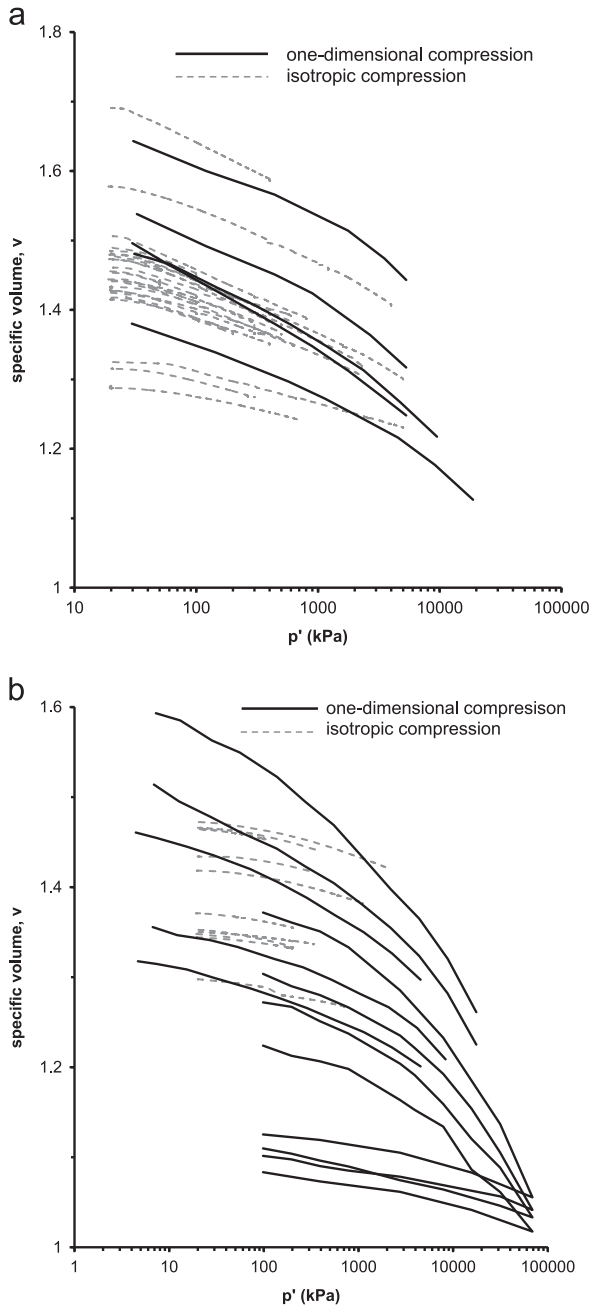

Fig. 3. Isotropic and one-dimensional compression data (oedometer data from Shipton and Coop, 2012). (a) SPF soil. (b) SNF soil.

data from the triaxial apparatus, p' has been estimated from $k_0 = 1 - \sin\phi'$. For the SNF soil, some of the oedometer tests were carried out in a high pressure floating ring oedometer that could reach a vertical stress of about 100 MPa. These data clearly show that even if the higher specific volume samples have steeper compression paths, the convergence of the paths from different initial specific volumes is not rapid enough for there to exist a unique normal compression line. Also, for the SPF soil, it is clear there is not sufficient space for there to be a unique normal compression line between the end of the tests and where the compression curves must approach an asymptote at $v = 1$.

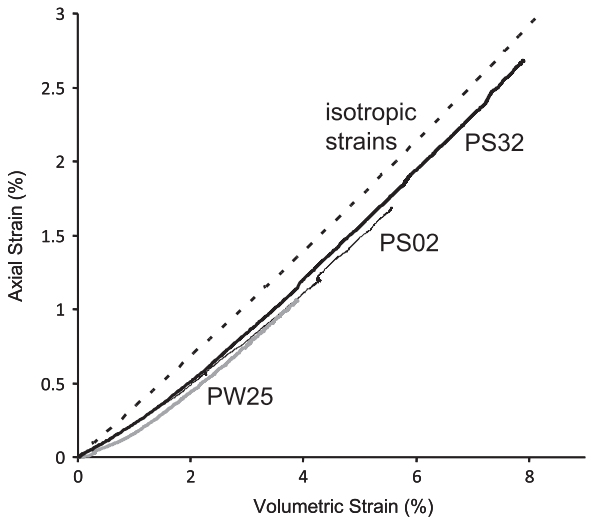

Fig. 4. Strains in three samples of the SPF soil during isotropic compression.

A similar pattern of lack of convergence to a unique normal compression line is seen for the isotropic compression data. As might be expected, the isotropic paths are flatter than those for one-dimensional compression, but even if some tests reached several MPa, this was not sufficient to observe the steepening that occurs in the one-dimensional paths at very higher stresses. A comparison of the two soils shows that the SNF soil has initially flatter compression paths, but that there is also greater curvature. No effect of the sample preparation method could be found in the data for either soil and no significant particle breakage occurred, so the steepening of the compression curves is not caused by the onset of breakage as it might be for a clean sand.

Throughout this paper, a conventional linear specific volume axis has been used. Butterfield (1979) proposed a logarithmic v axis, while Pestana and Whittle (1995) and McDowell (2005) used a logarithmic e (void ratio) axis. However, neither of these was found to be useful in detecting convergence towards unique normal compression lines.

Fig. 4 shows the strains that developed during isotropic compression for samples of the SPF soil. All three tests follow very similar paths, with axial strains that are initially smaller than the radial strains, but quickly tending towards isotropy of strain increments and following paths parallel to the isotropic line. This suggests that the differences in the locations of the compression paths in the v:lnp' plane do not have their seat in anisotropy of the samples. The data in Fig. 4 are based on the external measurements of axial and volumetric strain so that the isotropy of the strains also confirms that the effects of the end platen friction are not severe.

2.4. Shearing

Examples of stress–strain data for the tests are given in Figs. 5 and 6. The tests were all conducted to as large strains as the apparatus permitted, because large strains were required for both soils in order to approach a reasonably constant volume and stress state. For the tests that reached larger strains,

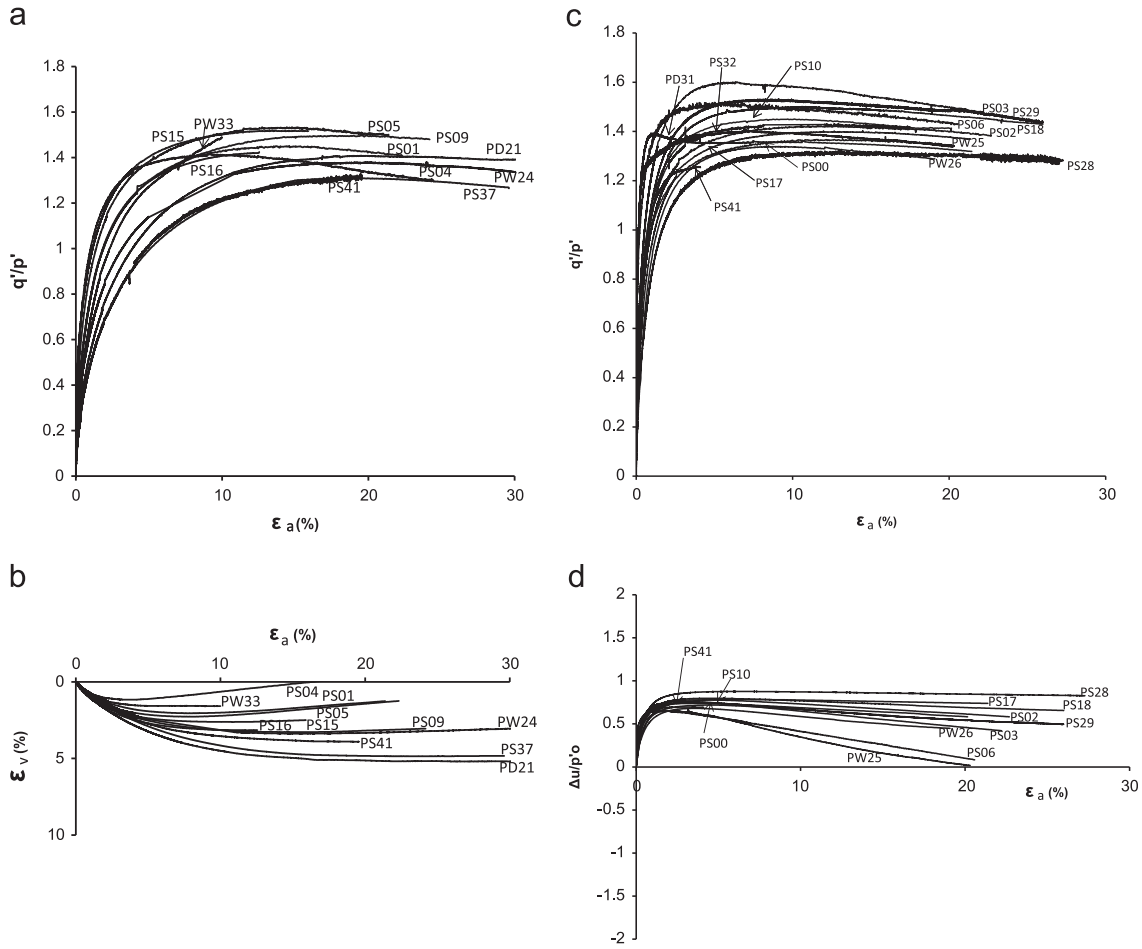

Fig. 5. Examples of stress–strain data for shearing of the SPF soil. (a) Drained tests, stress–strain data. (b) Drained tests, volume change data. (c) Undrained tests, stress–strain data. (d) Undrained tests pore pressure data (p'_0 is the initial value of p').

the stress and volume changes at the end of shearing were quite small in most cases. For some tests where the stresses and or volumetric strain were not quite constant at the end of shearing, a hyperbolic extrapolation to the critical state has been used, as will be discussed later. For other tests, notably the undrained tests on the SNF soil, where the tests are too incomplete to be extrapolated, the tests are indicated as "incomplete" on subsequent figures. All the undrained tests on the SNF soil had to be terminated before reaching a critical state, because the pore pressures became unreliable as they dropped towards zero at which point the transducer could no longer measure the pore pressure reliably.

While the tests at medium to high stresses were compressive, the SPF soil was dilative at the lowest stress levels, even if most samples were sheared from states that were "normally consolidated" in the sense that they were currently at their maximum consolidation stress. In general, the SNF soil was more dilative than the SPF.

The stress paths and estimates of the critical state lines in the q:p' plane are given in Fig. 7. For the SPF soil, the chosen critical state line has a gradient $M=1.30$ and for the SNF, it is 1.36, corresponding to critical state angles of shearing resistance ϕ'_{cs} of 32.3° and 33.7°, respectively. The value for the SPF soil is close to the ϕ'_{cs} of 33° for the sand fraction (Takahashi and Jardine, 2007) and seems to be little influenced by the much lower ϕ'_{cs} of 23° of the kaolin content. Although a single value for M has been chosen for the SPF soil, M seems to be slightly lower for the higher pressure tests (Fig. 7a) than at lower stress levels (Fig. 7b), perhaps indicating a slight curvature of the critical state line and giving rise to some scatter in the final state in Fig. 5.

If soils have a unique critical state, then specimens of the same initial specific volume that are sheared undrained, from different initial values of p', will reach the same p' at the critical state. Typical data for the undrained shearing of the SPF soil are given in Fig. 8a. Three pairs of tests at similar specific volumes have been chosen, PW25 and PW26 ($v=1.23$–1.24), PS14 and PS19 ($v=1.41$) and PS08 and PS40 ($v=1.44$–1.46). Although there is some reduction in the difference in log p' for each pair of tests, they do not converge to a unique value. The values for p' were generally reasonably stable at the ends of the tests, although large strains were required in some cases. In two tests (PW25 and PW26), p' was not quite stable when the tests were ended, and hyperbolic extrapolations have been used. These extrapolations give similar curves to other tests, such as PS18, where larger

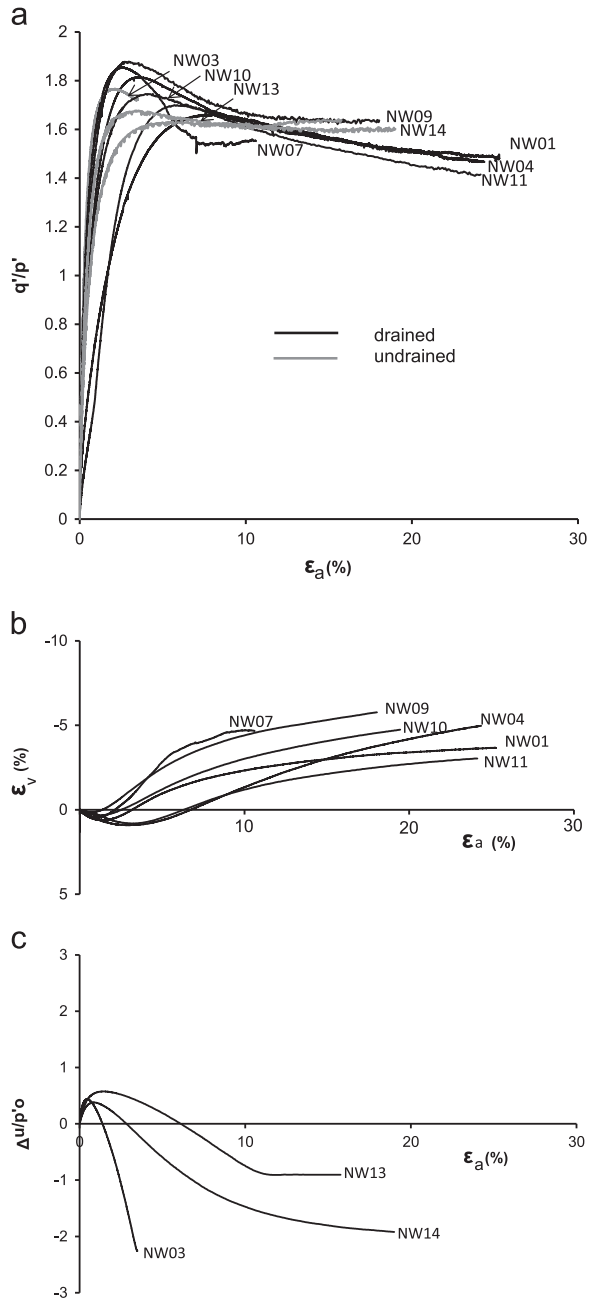

Fig. 6. Stress–strain data for shearing of the SNF soil. (a) Stress–strain data. (b) Drained tests, volume change data. (c) Undrained tests pore pressure data (p'_0 is the initial value of p').

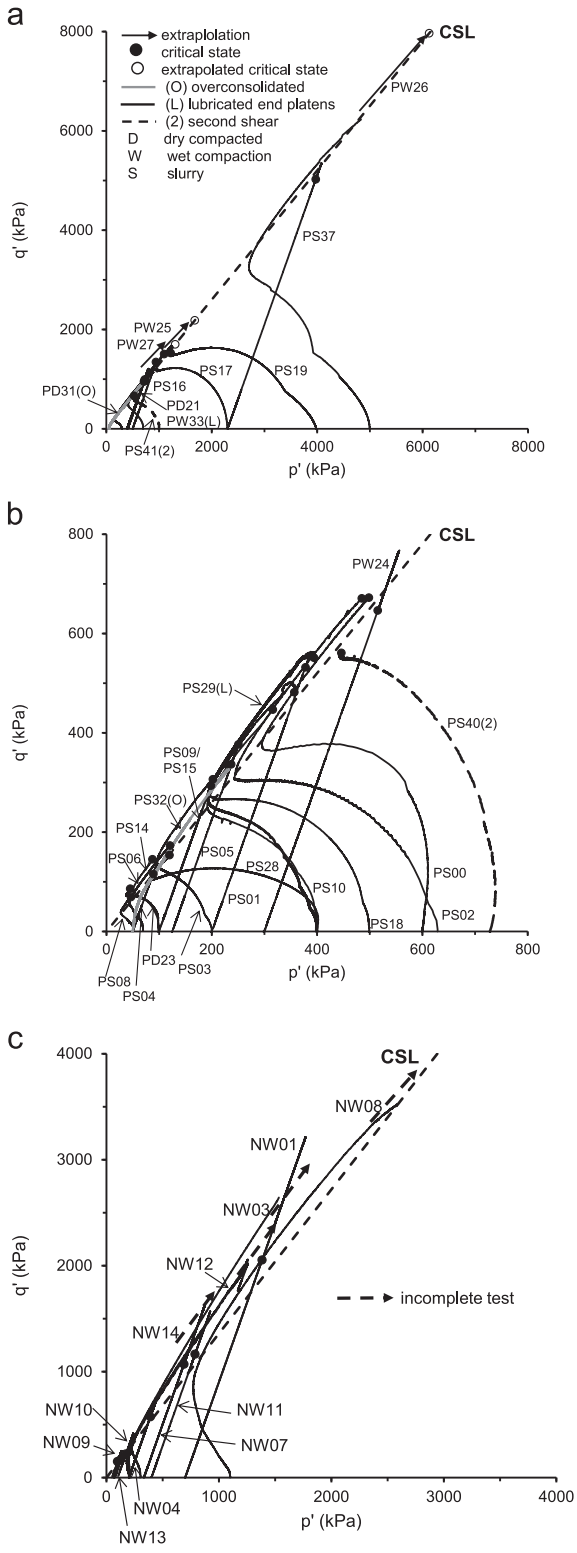

Fig. 7. Stress paths during shearing. (a) SPF soil, high pressures. (b) SPF soil lower pressures. (c) SNF soil.

strains had been reached and have little effect on the lack of convergence. A similar extrapolation was applied to one other undrained test, PW27.

In Fig. 8a, two tests are shown for identical samples at the same initial specific volume, one with lubricated end platens (PS29) and one without (PS18). While there is some slight influence of lubricating the ends, the effect is small relative to the large differences in final p' seen for the other tests.

Two different sample preparation techniques were used for the samples in the comparisons of Fig. 8a, but the same sample preparation technique was used within each pair that is compared. Thus, the lack of convergence cannot be attributed to comparisons between the different sample types. It is also not a feature only of one preparation method. The very slow

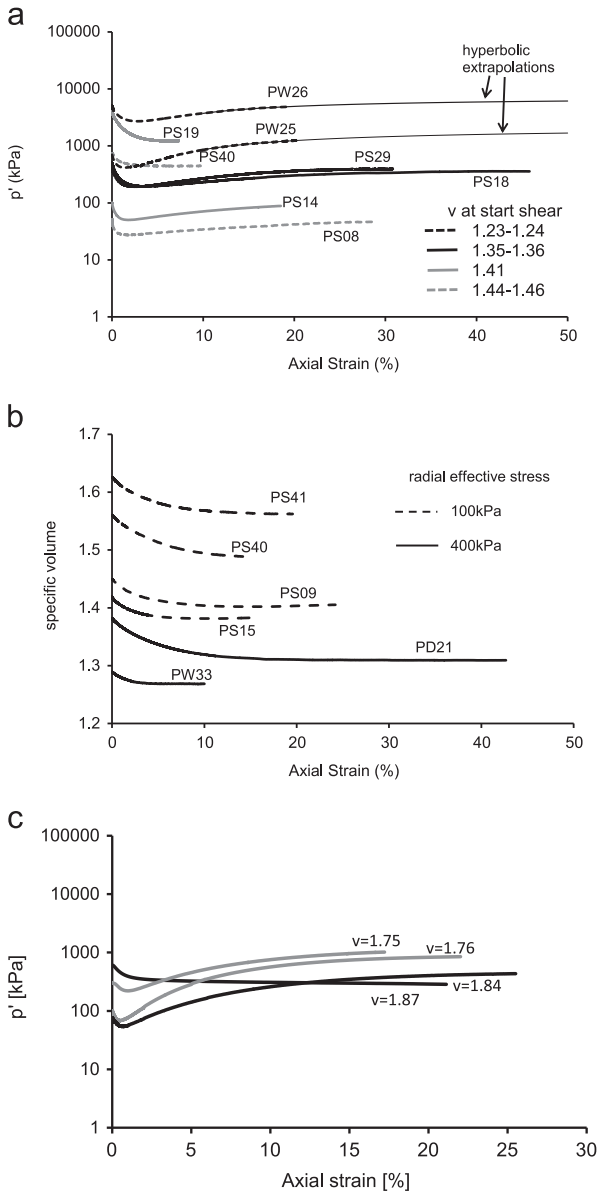

Fig. 8. Examples of non-convergence of states during shearing. (a) SPF soil, undrained tests. (b) SPF soil, drained tests. (c) Undrained tests on sand from Stava tailings (data taken from Carrera et al., 2011).

rate of change in p' at the end of the tests or extrapolations is an indication that the lack of convergence is not related to incomplete testing, but that a unique volume, if it is attainable, could only be reached by very different forms of loading, emphasising that while the correct definition for the critical state should include a unique fabric, it may be of quite academic interest for these soils in simple monotonic loading.

For constant radial effective stress drained tests, a unique critical state line would mean that specimens of different initial specific volumes at the same initial p' should converge to the same final v, but again Fig. 8b indicates that this is far from the case. While there is some decrease in the differences in v from the initial values, the final differences remain very large. The values for the specific volume at the ends of the tests are reasonably stable, so no extrapolations were necessary. It is again clear that the lack of convergence does not simply result from incomplete shearing. When assessing the convergence, or lack of it, it is important to understand how significant the differences in v are relative to the accuracy of their measurement. To this end, it is crucial that the accuracy of the specific volume is actually established, as has been done here, rather than simply estimated. The triaxial tests had a mean error of v of about ± 0.005, which is less than 3% of the final difference in v between tests PS15 and PS41.

Apparently unique critical states have been demonstrated for many mixtures of sands with fines (e.g., Murthy et al., 2007), but close examination of the data often reveals that the range in initial specific volumes tested was insufficient to tell whether, within the scatter of critical state data obtained, the behaviour is transitional or not. One study that intentionally did test a wide range in initial states was that by Carrera et al. (2011), on sands and silty sands from the Stava tailings, since early indications had been that the soils might be transitional. The tests were mostly conducted in the same laboratory as the work described in this paper using similar procedures. Ultimately, the research revealed that there was no transitional behaviour for any of the sand–silt mixtures investigated and that each gave a unique critical state line. Fig. 8c gives typical undrained test data from the clean sand. The two pairs of tests at different initial values of v clearly show very much better convergence than in Fig. 8a, the small remaining differences at the critical state in this case being largely attributable to the initial differences in v.

2.5. Critical states in the v:lnp' plane

The end of test states, including extrapolations when applied, have been plotted in the v:lnp' plane in Fig. 9 along with the paths followed during isotropic compression and shearing. For the most incomplete tests, particularly the undrained tests on the SNF soil, no extrapolations were possible and the directions of movement when the tests were terminated are indicated with an arrow. Each soil shows a very wide range in critical state locations and neither has a unique critical state line.

In Fig. 9b, five groups (A–E) of samples of the SPF soil have been identified that have similar initial specific volumes. Accepting the conclusion of Ferreira and Bica (2006) that parallel critical state lines can exist for transitional soils, a set of parallel lines has been chosen that fit the data well. The gradient chosen for these critical state lines was 0.047, based on the data from these groups and others not shown for clarity. Here, the tests had all been sheared to more stable states than some of those reached by the tests of Ferreira and Bica (2006), and a much greater range in initial values of v was used, so these data add significant strength to their hypothesis. There is no evidence of any curvature of these critical state lines at lower stresses, as seen for many sands (e.g., Verdugo and Ishihara, 1996) or silts (e.g. Carrera et al., 2011). This family of critical state lines indicates that the initial specific volume controls the location of the current critical state line, and the means of that influence can only be through the fabric, even if clear differences could not be observed in the SEM.

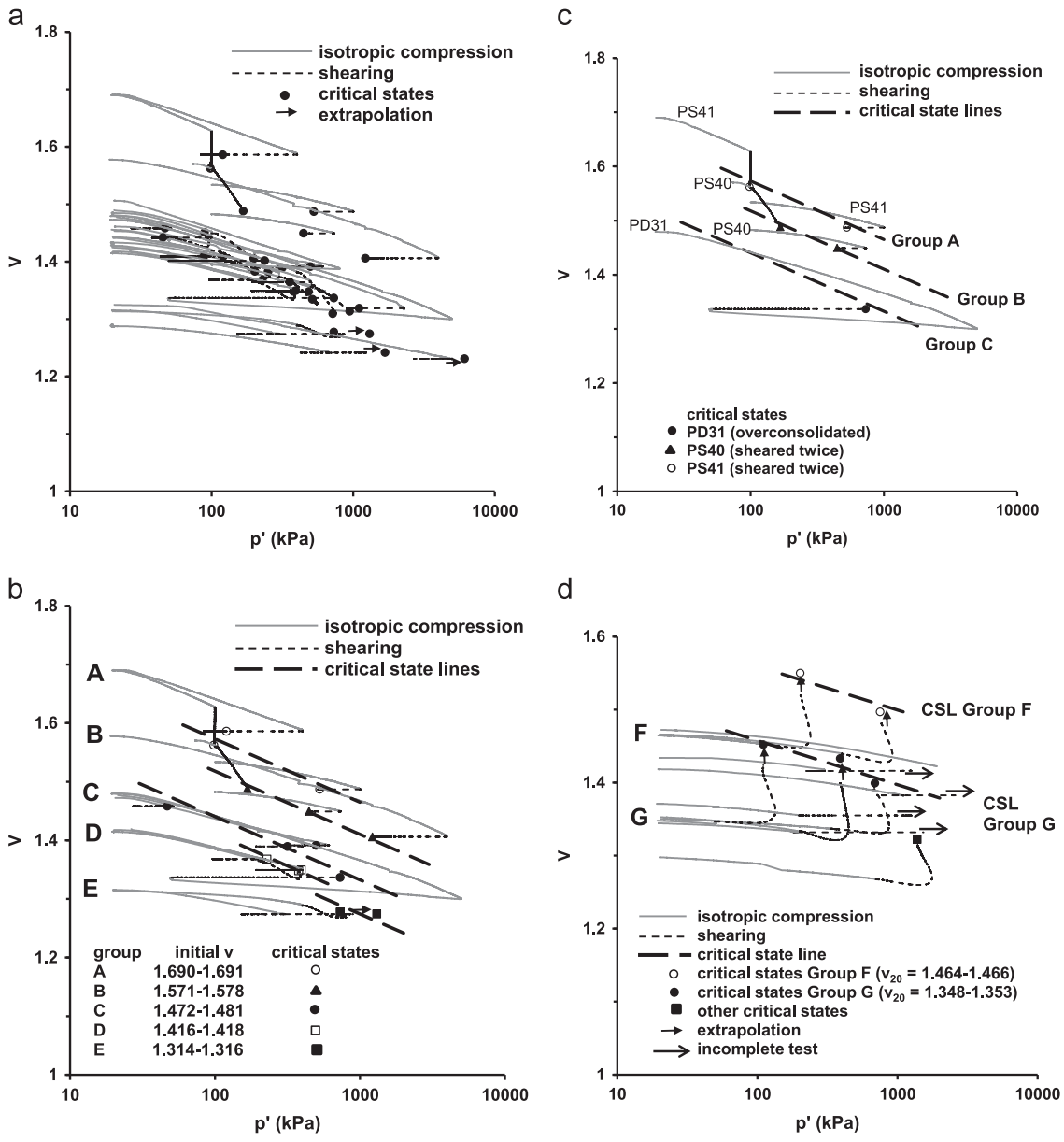

Fig. 9. Critical states in the volumetric plane. (a) SPF soil, all data. (b) SPF soil, selected initial specific volumes. (c) Details of tests PD31, PS40 and PS41, SPF soil. (d) SNF soil.

There has been considerable work carried out on soils of mixed particle size considering how a modified form of void ratio, such as an inter-granular void ratio, can give a unique critical state line for different gradings (e.g., Thevanayagam and Mohan, 2000). However, if the critical state line is non-unique in the v:lnp' plane, then no modification to the specific volume can make it unique.

The overconsolidated samples are especially interesting (PD31 and PS32), because the other SPF tests all approach the critical state line from the wet side. They were sheared from $p'_0 = 50$ kPa at overconsolidation ratios of 100 and 16, respectively. These tests had three purposes, namely, (1) to check how robust the critical state lines are and whether overconsolidation might change the line the soil moved towards, (2) if incomplete testing were a problem, then shearing a specimen from the dry side would identify a lower critical state line location, and (3) if the use of non-lubricated ends were preventing the samples from reaching unique critical state lines, then the overconsolidated samples would again come to a critical state below that for samples sheared from the wet side. Test PS31 had a v_{20} of 1.479, but was over-consolidated by unloading isotropically from 5000 kPa to 50 kPa in the high pressure triaxial apparatus, so that its overconsolidation ratio was 100. Its critical state plots only very slightly below the critical state line chosen for the specimens within the range of v_{20} 1.472–1.481 (see Fig. 9c, Group C), which can be attributed to some observed localisation of strains, as might be expected for such a high degree of overconsolidation. However, there is no tendency for this test to reach a significantly lower critical state line location, which

indicates that the different critical state lines cannot be a result of any simple incompleteness of shearing, at least in triaxial compression, nor can the use of frictional ends be a significant issue and that the differences of initial specific volume are not easily changed, as was evident in Fig. 8.

Tests PS40 and PS41 were also designed to see how robust the critical state lines are. They were first sheared drained at 100 kPa and then recompressed to the higher isotropic stress levels of 729 kPa and 1000 kPa, respectively, as shown in Fig. 9c, where they were sheared undrained. The sample shapes after the first shearing were not significantly barrelled because the volumetric strains had been compressive. For the second shearing, the critical states plot very close to the same critical state lines as were reached for the first shearing (Group B for PS40 and Group A for PS41). As for the overconsolidated samples, these tests again confirmed that the influence of the initial specific volume cannot be easily broken down.

The non-convergence of the critical states is perhaps not as surprising as it might initially appear. The high pressure oedometer tests apply volumetric strains to the SPF soil of the order of 12–18% and shear strains of 8–12%. The volumetric strains in the triaxial tests which are at lower stress levels are more varied, at around 1–12%, and the shear strains are typically in the order of 15–30%. The fairly similar magnitudes of strains would lead us to expect that there would not be unique final critical state volumes in the triaxials if the oedometer compression curves do not converge completely. At the highest stress levels, the oedometer curves are still converging slowly in Fig. 3a, but for the triaxial tests, continued shear strain gives rise to the negligible convergence of the critical states in Fig. 8, which might indicate that these very stable forms of fabric that cause transitional behaviour are much less easily broken down by shear strain than by volumetric strain. In the constitutive modelling of structured soils, more emphasis is usually given to the effect of volumetric strain in destructuration than to shear strain (e.g., Callisto et al., 2002; Koskinen et al., 2002), and some models have damage functions that are solely related to volumetric strains (e.g., Lagioia and Nova, 1995; Baudet and Ho, 2004). Generally, the maximum importance of shear strains to destructuration is to allow the effect to be equal to that of the volumetric strains (e.g., Baudet and Stallebrass, 2004; Gajo and Wood, 2001).

For the SNF soil, there are fewer tests, although the patterns of behaviour are very similar and the assumption of a family of parallel critical state lines in Fig. 9d is consistent with the data. There is also greater incompleteness in some tests. For some of the drained tests, small hyperbolic extrapolations were again made as indicated, but the undrained tests were too incomplete to allow this. Reaching a critical state in undrained loading would be especially difficult for this soil because of the very large reduction in pore pressure that would be needed. The gradient λ of 0.026 the critical state lines is much lower than that for the SPF soil which has a λ of 0.047. The smaller amount of data and the less complete nature of these tests mean that the conclusion of the non-unique critical state lines cannot be as firmly established as for the SPF soil. Even if the visible localisation was not severe, it is inevitably an issue with dilative tests and very high pressures would be required to bring these samples to compressive states. Nevertheless, the patterns of behaviour seem very similar and the hypothesis of the non-unique critical state lines is confirmed by the fact that the total amount of dilation and the rate of dilation seem unrelated to the initial volume of the soil. In Fig. 10, the maximum rates of dilation are plotted against the initial state parameter (Wroth and Bassett, 1965; Been and Jefferies, 1985), where the state parameter, ψ, is defined as the difference between the current specific volume and that on the critical state line at the current p' ($\psi = v - v_{cs}$). In Fig. 10a, the assumption is made that the critical state lines are those shown in Figs. 9d and in Fig. 10b that there is one critical state line corresponding to the uppermost line in Fig. 9d. The assumption of a unique line seems unlikely to be correct since it gives similar rates of dilation at very different state parameters, while the relationship in Fig. 10a seems reasonable.

For both soils, at higher stress levels and for looser samples, the isotropic compression paths tend to move outside the corresponding critical state line and tend to become parallel to it. It is clear from Fig. 3, however, that at very high stress levels, the one-dimensional compression paths become significantly steeper, which may be an indication that the critical state lines may do too, but very high pressure tests would be needed to verify this.

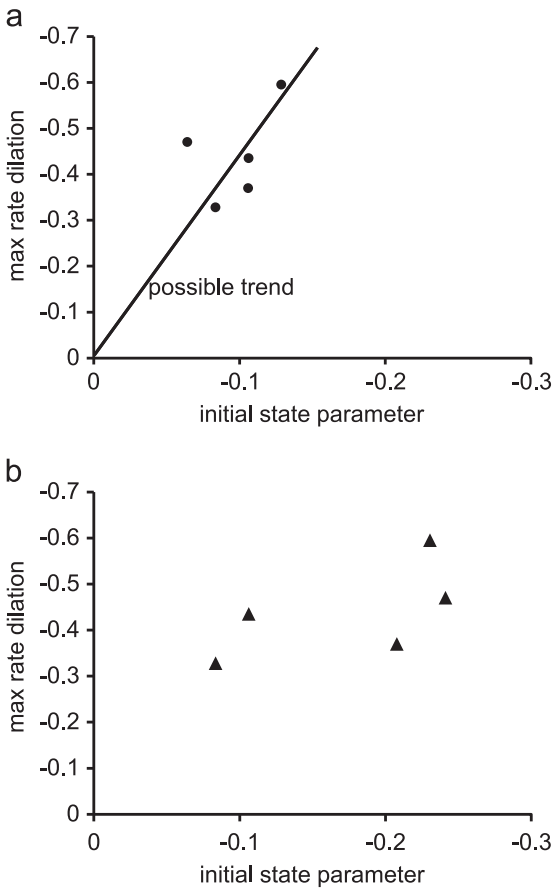

Fig. 10. Influence of initial state on maximum rate of dilation for SNF soil. (a) Assuming multiple critical state lines. (b) Assuming a single critical state line.

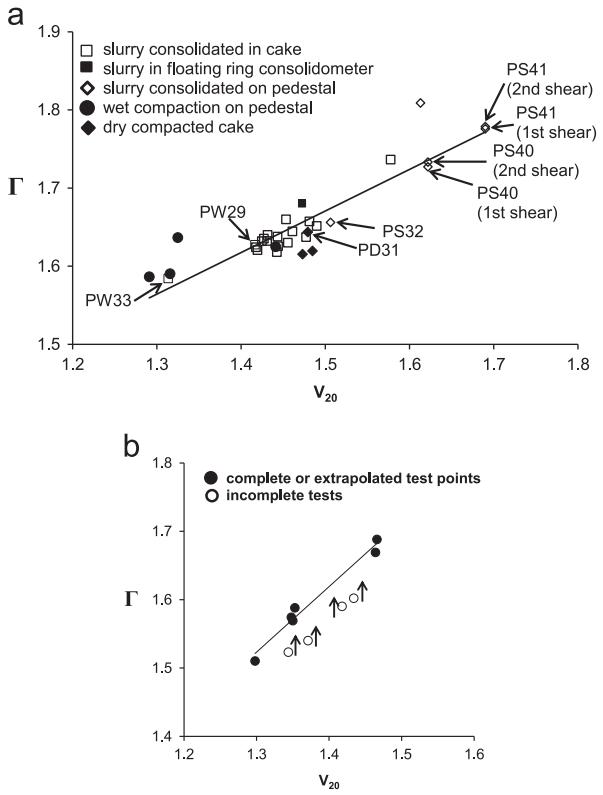

Fig. 11. Influence of initial specific volume, v_{20}, on critical state line intercept, Γ. (a) SPF soil. (b) SNF soil.

Assuming that the hypothesis of a family of parallel critical state lines for each soil is correct, a correlation is made in Fig. 11 between the initial specific volume, v_{20}, and the projected intercepts of the critical state lines at 1 kPa, Γ. Here a separate critical state line was assumed for every single test rather than grouping them into ranges of values of v_{20}. With some data scatter, unique relationships are obtained for each soil between Γ and v_{20}. If the assumption of parallel critical state lines were not correct, then this would not be the case. The gradients of the regression trend lines are 0.52 and 0.97 for the SPF and SNF soils, respectively.

For the SPF soil, a variety of sample preparation methods was used to achieve the greatest range in values of v_{20}, but where the data for different methods overlap, it is evident that they give similar data, indicating that the preparation method is only important for the critical states of this soil through the value of v_{20} that it creates. The use of lubricated end platens does not significantly affect the data either, since Tests PS29 and PW33 with lubricated ends, plot on the same trend as the other tests without. The data points for the two overconsolidated specimens, PD31 and PS32, again plot close to the same trend line, confirming that approaching the critical state lines from the dry side does not significantly change their apparent location. As discussed above, this also indicates that the non-unique critical state lines cannot be the result of using frictional ends. The second shearing points for tests PS40 and PS41 plot very close to the first shearing points and the trend line, indicating that recompression and second shearing of the same specimen has no effect on the critical state line that it reaches.

2.6. Normalisation of shearing data

Several forms of normalisation of the shearing data were attempted. The first, used only for the SPF soil, was to take equivalent pressures on the compression paths, assuming that each path represented an individual normal compression line. These were assumed to be straight and parallel and passing through the maximum consolidation stress reached. The equivalent pressure is then

$$p'_e = \exp\left(\frac{N-v}{\lambda}\right) \tag{5}$$

where N is the projected intercept of the normal compression line at 1 kPa. The result, shown in Fig. 12a for the SPF soil, is unsuccessful with critical states that do not define a unique point and with no evidence of any unique boundary surface.

When an equivalent pressure is taken on the individual critical state lines, the definition is

$$p'_{cs} = \exp\left(\frac{\Gamma-v}{\lambda}\right) \tag{6}$$

The resulting normalisation in Fig. 12b forces all the critical states to plot at $p'/p'_{cs}=1$, and the resulting plot is much more successful with a clear state boundary surface (SBS) on the dry side (Hvorslev surface), and possible evidence of one on the wet side, although again it seems that tests at even higher pressures than the 5 MPa used here would be needed to define it accurately. The difficulty of defining the wet side is accentuated by the wide separation of the isotropic intercept of the state boundary surface from the critical state line, as Ferreira and Bica (2006) also observed for a transitional soil. The agreement between the normalised test paths for different values of v_{20} again confirms the hypothesis of an infinite number of parallel critical state lines, and that the behaviours of samples of any initial specific volume are similar provided that the basis of comparison is the current state (v, p') relative to the appropriate critical state line. While there are differences in the normalised paths of drained and undrained tests, no clear effects of the sample preparation method can be seen.

A state parameter normalisation is shown for the SPF soil in Fig. 12c, again assuming individual critical state lines for each v_{20}. The technique is not any more helpful, since the same doubts apply about whether or not the stress levels have been high enough to locate the wet side state boundary surface, while the dry side is not as well defined as for the equivalent pressure normalisation in Fig. 12b.

The normalisation using an equivalent pressure on individual critical state lines is shown in Fig. 12d for the SNF soil. Only the dry side boundary is defined and extremely high pressure tests would be required to reach the wet side.

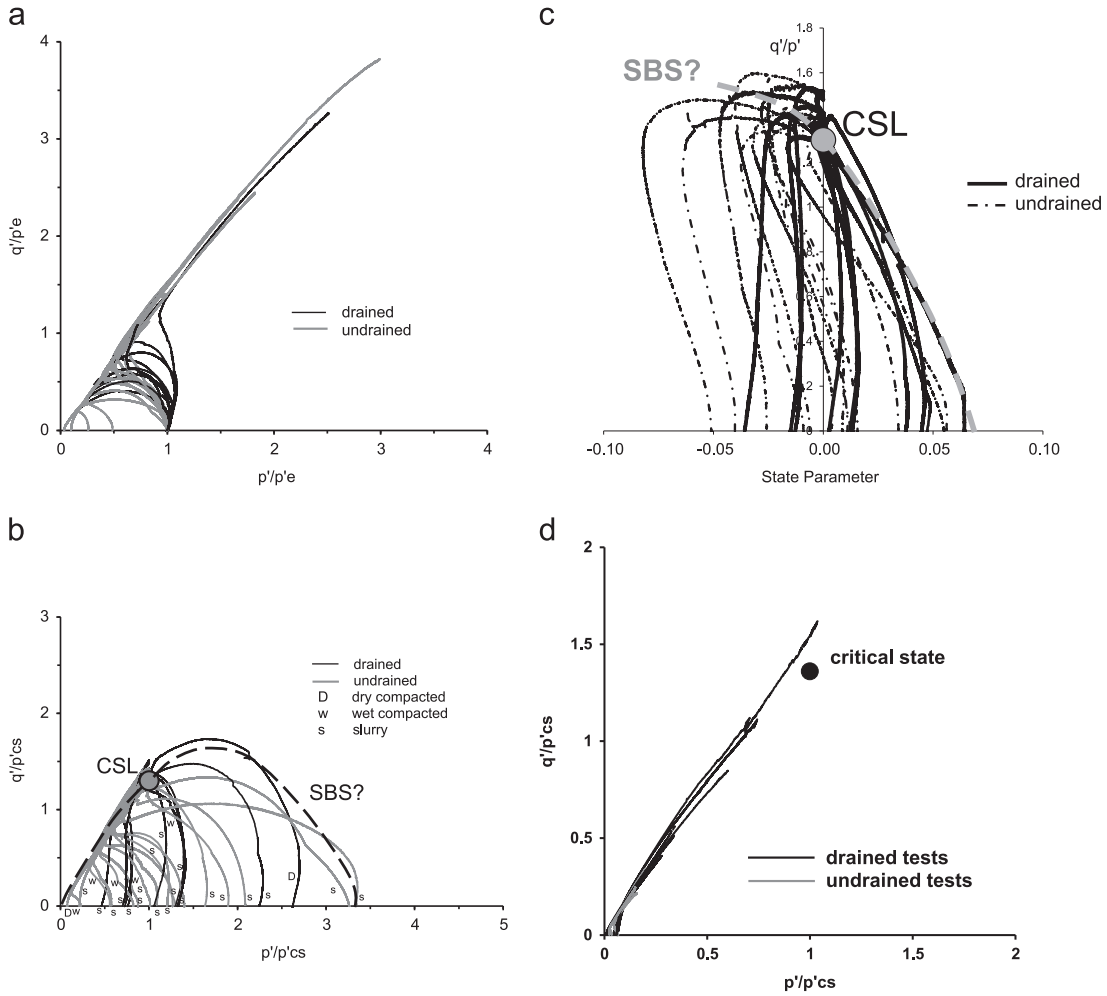

Fig. 12. Normalised stress paths during shearing. (a) SPF soil, equivalent pressure taken on individual normal compression lines. (b) SPF soil, equivalent pressure taken on individual critical state lines (s slurry sample, w wet compacted, D dry compacted). (c) Normalisation for SPF soil using state parameter. (d) SNF soil, equivalent pressure taken on individual critical state lines.

2.7. Final particle size distributions

The initial particle size distributions in Fig. 1 were measured using the usual techniques of wet sieving and sedimentation. Particle size distributions of the fraction above 63 μm were also measured for the two soils before and after various tests using a laser scanning particle analyser, which has been found to be better able to highlight small changes in grading (Altuhafi and Coop, 2011). The particle size distributions of the coarse fractions from the particle analyser are shown in Fig. 13. Within the slight scatter of the data, there is no evidence of any significant particle breakage as would be typical for sands (e.g., Ghafghazi et al., 2014). For the SPF soil, the test that would be expected to be the most prone to breakage would be PS37, which was a drained constant radial stress test at an effective confining pressure of 2.3 MPa, but it is clear that there is none, which is perhaps surprising given that 75% of the sample is sand. For the SNF soil, the gradings have only been measured for oedometer samples, but test NOW03 shows that even with a vertical stress of 27.7 MPa,

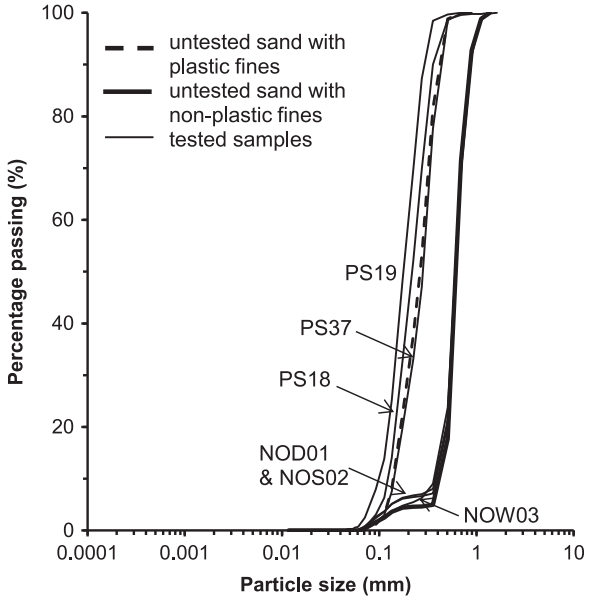

Fig. 13. Particle size distributions of coarse fractions after testing.

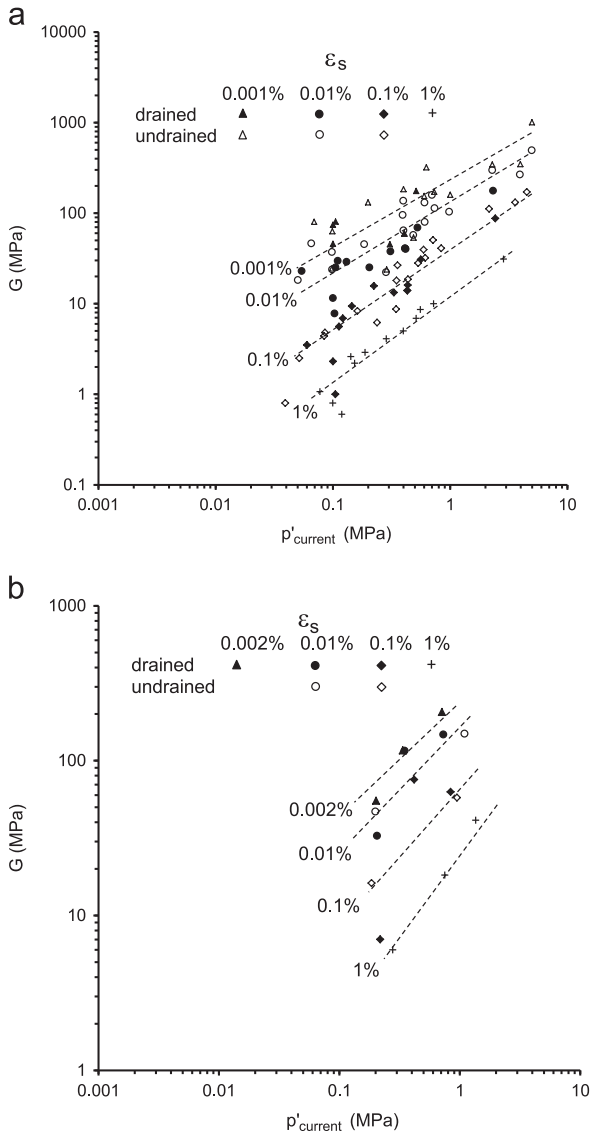

Fig. 14. Stiffnesses of the two soils. (a) SPF soil. (b) SNF soil.

there has been no significant breakage. Again, this is perhaps unexpected given the high proportion of sand and the fact that the fine particles are also clastic.

2.8. Stiffnesses

The tangent stiffnesses from the shearing stages in Fig. 14 have been calculated from linear regressions through short sections of the stress–strain curves. The calculation of the shear strains has been based on the local axial strains and for the drained tests the local radial strains if they were measured, or data from the volume gauge if they were not. These calculations assume the soil behaviour to be isotropic. Data are only shown for normally consolidated specimens meaning samples at the maximum p' they have experienced.

Within some data scatter, there is little difference between the drained and undrained tests and no consistent differences were found for different sample preparation techniques either.

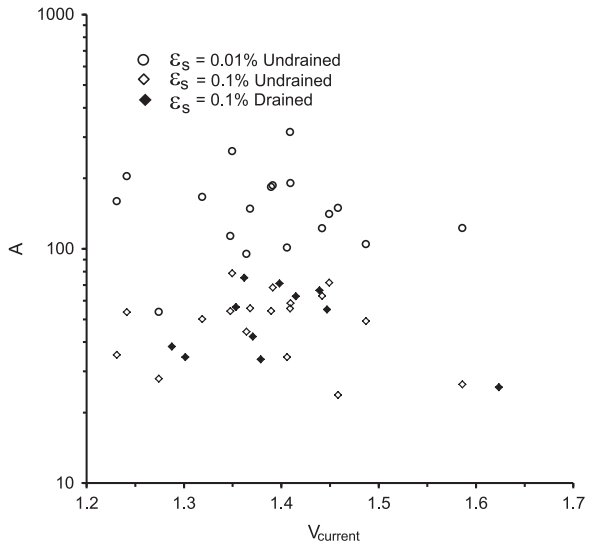

Fig. 15. Values of A for two strain levels for the SPF soil.

The data can be interpreted with a pattern of convergent contours for increasing strain levels, as observed by Viggiani and Atkinson (1995) for clays or Jovicic and Coop (1997) for uniform sands on their normal compression lines. Similarly to what these authors have observed, the lines might be represented by equations of the form $G=Ap'^{n}$, with the values for A decreasing with the strain level while n increases.

For most soils, the current volume would play a key role in the stiffness, as has been emphasised, for example, by Viggiani and Atkinson (1995) for clays, Jovicic and Coop (1997) for sands and Salgado et al. (2000) for silty sands, but that seems not to be the case for this soil. For elastic stiffnesses, a common means of normalising for different volumes is to use the function $e^{-1.3}$, as proposed by Jamiolkowski et al. (1994). In Fig. 15, values for A are plotted against the current specific volume for each test on the SPF soil at strain levels of 0.01% and 0.1%. The drained test data at 0.01% have been omitted as they were too scattered. These individual values for A for each test have been calculated assuming that the value for n is common to all tests for each strain level. For this range in values for v, a decrease in stiffness by a factor of around 3.5 would be expected if the elastic $e^{-1.3}$ function were used. Here, the strain levels are larger than the elastic range, but it is debatable whether or not the data would support any effect of volume on the stiffness at all. For the SNF soil, the data are sparser, but in Fig. 14b, there is little scatter of the data considering the large differences in specific volume of the samples and again no consistent effects of density could be found. The stiffness of these transitional soils in normally consolidated states is therefore predominantly a function of the stress level, while the specific volume seems to have little influence.

3. Conclusions

The SPF soil mixture showed a clear transitional behaviour, in which the current specific volume in both compression and

shearing was dependent on the initial specific volume. The work confirmed the hypothesis of Ferreira and Bica (2006) that the end of test states can be represented by a family of parallel critical state lines and state boundary surfaces. The new data add significant strength to this hypothesis primarily by showing similar data for two new soils, but also through the tests being more complete and also not having the differences in initial grading of the soils Ferreira and Bica tested. A much greater range in initial densities has also been used, giving clear relationships between critical state line intercept Γ and the initial specific volume. While the data for the SNF soil were less extensive, the patterns of behaviour were very similar to those of the SPF soil, confirming that transitional behaviour need not be related to the plasticity of the fines.

Greater confidence in this framework was also given by the use of lubricated end platens in two tests, which did not significantly affect the data in the v:lnp' plane, and by the use of heavily overconsolidated samples and samples sheared twice from different stress levels, which demonstrated the family of critical state lines to be robust and not easily changed. Although Ferreira and Bica (2006) only used one preparation technique for their remoulded triaxial specimens, a variety of techniques was used here, showing that the preparation method did not affect the relationship between Γ and the initial specific volume. Additionally, it has been found that since the strains were isotropic, the fabric that causes the transitional behaviour is not an anisotropic one. An examination of the final gradings revealed that neither soil showed significant particle breakage. The current work also examined the small strain behaviour showing that, for these transitional soils, there was no significant effect of the initial specific volume of the sample on its stiffness at a given stress level for normally consolidated states.

The steepening and eventual slow convergence of the oedometer compression curves at extremely high pressures may be an indication that the assumption of parallel critical state lines and state boundary surfaces that has been found for stresses up to 4 MPa, may break down at even higher stresses. The differences in fabric that sustain the different specific volumes at these critical states identified in triaxial compression may also break down more quickly under more complex stress paths or at extremely large strains. Finding transitional behaviour in two simple soils now enables the research community to create easily similar soils with transitional behaviour for further work.

Acknowledgements

The topic of this paper has been a controversial one throughout the review process, and the authors would like to sincerely thank Soils and Foundations for their persistence and guidance with the paper through its many revisions, so much in contrast to the “Flat Earth Society”. We would welcome a robust debate about its content. The authors are grateful to Thomas Hui and Rachel Skeete who carried out some of the tests, to Dr. Pedro Ferriera for his help in replying to the reviewers’ comments and to Dr. Alessandra Carrera for her help with the analysis of the Stava tailings sand data. The work described in this paper was partially supported by a grant from the Research Grants Council of the Hong Kong Special Administrative Region, China (Project no. CityU 112911).

References

Altuhafi, F.N., Baudet, B.A., Sammonds, P., 2010. The mechanics of subglacial sediment: an example of new “Transitional” behaviour. Can. Geotech. J. 47 (7), 775–790.

Altuhafi, F., Coop, M.R., 2011. Changes to particle characteristics associated with the compression of sands. Géotechnique 61 (6), 459–471.

Atkinson, J.H., Fookes, P.G., Miglio, B.F., Pettifer, G.S., 2003. Destructuring and disaggregation of Mercia Mudstone during full-face tunnelling. Q. J. Eng. Geol. Hydrogeol. 36, 293–303.

Baudet, B.A., Ho, E.W.L., 2004. On the behaviour of deep-ocean sediments. Géotechnique 54 (9), 571–580.

Baudet, B., Stallebrass, S., 2004. A constitutive model for structured clays. Géotechnique 54 (4), 269–278.

Been, K., Jefferies, M., 1985. A state parameter for sands. Géotechnique 35 (2), 99–112.

Burland, J.B., Symes, M., 1982. A simple axial displacement gauge for use in the triaxial apparatus. Géotechnique 32 (1), 62–65.

Butterfield, R., 1979. A natural compression law for soils (an advance on e–logp'). Géotechnique 26 (4), 469–480.

Callisto, L., Gajo, A., Wood, D.M., 2002. Simulation of triaxial and true triaxial tests on natural and reconstituted Pisa clay. Géotechnique 52 (9), 649–666.

Carraro, J.A.H., Prezzi, M., 2008. A new slurry-based method of preparation of specimens of sand containing fines. Geotech. Test. J. 31 (1), 1–11.

Carrera, A., Coop, M.R., Lancellotta, R., 2011. The influence of grading on the mechanical behaviour of Stava tailings. Géotechnique 61 (11), 935–946.

Chen, Y.C., Chuang, J.C., 2001. Effects of fabric on steady state and liquefaction resistance. In: Proc. 11th Int. Offshore and Polar Engng. Conf., Stavanger: 524–529.

Chu, J., Leong, W.K., Loke, W.L., 2003. Discussion of “Defining an appropriate steady state line for Marriespruit gold tailings”. Can. Geotech. J. 40, 484–486.

Coop, M.R., Cotecchia, F., 1995. The compression of sediments at the archaeological site of Sibari. In: Proc. 11th ECSMFE, Copenhagen, 8, 19-26.

Cotecchia, F., Chandler, R.J., 2000. A general framework for the mechanical behaviour of clays. Géotechnique 50 (4), 431–447.

Cuccovillo, T., Coop, M.R., 1997. The measurement of local axial strains in triaxial tests using LVDTs. Géotechnique 47 (1), 167–171.

Duong, T.V., Tang, A.M., Cui, Y.-J., Trinh, V.N., Dupla, J.-C., Calon, N., Canou, J., Robinet, A., 2013. Effects of fines and water contents on the mechanical behavior of interlayer soil in ancient railway sub-structure. Soils Found. 53 (6), 868–878.

Fearon, R.E., Coop, M.R., 2000. Reconstitution: what makes an appropriate reference material? Géotechnique 50 (4), 471–477.

Ferreira, P.M.V., Bica, A.V.D., 2006. Problems in identifying the effects of structure and critical state in a soil with a transitional behaviour. Géotechnique 56 (7), 445–454.

Fourie, A.B., Papageorgiou, G., 2001. Defining an appropriate steady state line for Merriespruit gold tailings. Can. Geotech. J. 38 (4), 695–706.

Gajo, A., Wood, D.M., 2001. A new approach to anisotropic, bounding surface plasticity: general formulation and simulations of natural and reconstituted clay behaviour. Int. J. Numer. Anal. Methods Geomech. 25 (3), 207–241.

Ghafghazi, M., Shuttle, D.A., DeJong, J.T., 2014. Particle breakage and the critical state of sand. Soils Found. 54 (3), 451–461.

Jamiolkowski, M., Lancellotta, R., Lo Presti, D.C.F., 1994. Remarks on the stiffness of six Italian clays. In: Proc. First Int. Conf. on Pre-failure Deformation Characteristics of Geomaterials, Hokkaido, 855–885.

Jovicic, V., Coop, M.R., 1997. The stiffness of coarse grained soils at small strains. Géotechnique 47 (3), 545–561.

Koskinen, M., Karstunen, M., Wheeler, S.J., 2002. Modelling destructuration and anisotropy of a soft natural clay. In: Proc. Fifth Eur. Conf. Numer. Methods Geotech. Engng, Paris, pp. 11–20.

Lagioia, R., Nova, R., 1995. An experimental and theoretical study of the behaviour of a calcarenite in triaxial compression. Géotechnique 45 (4), 633–648.

La Rochelle, P., Leroueil, S., Trak, B., Blais-Leroux, L., Tavenas, F. (1988) Observational approach to membrane and area corrections in triaxial tests. In: Advanced Triaxial Testing of Soil and Rock. Donaghe, R.T., Chaney, R.C., Silver, M.L. (Eds.), pp. 715–731.

Liu, M.D., Carter, J.P., 2002. A structured cam clay model. Can. Geotech. J. 39, 1313–1332.

Martins, F., Bressani, L.A., Coop, M.R., Bica, V.D., 2001. Some aspects of the compressibility behaviour of a clayey sand. Can. Geotech. J. 38 (6), 1177–1186.

Martins, J.P., 1983. Shaft Resistance of Axially Loaded Piles in Clay (Ph.D. Thesis). University of London.

McDowell, G.R., 2005. A physical justification for log$e$–logσ based on fractal crushing and particle kinematics. Géotechnique 55 (9), 697–698.

McDowell, G.R., Bolton, M.D., 1998. On the micro mechanics of crushable aggregates. Géotechnique 48 (5), 667–679.

Murthy, T.G., Loukidis, D., Carraro, J.A.H., Prezzi, M., Salgado, R., 2007. Géotechnique 57 (3), 273–288.

Nocilla, A., Coop, M.R., Colleselli, F., 2006. The mechanics of an Italian silt; an example of "Transitional" behaviour. Géotechnique 56 (4), 261–271.

Nougier-Lehon, C., Vincens, E., Cambou, B., 2005. Structural changes in granular materials: the case of irregular polygonal particles. Int. J. Solids Struct. 42 (24–25), 6356–6375.

Pestana, J.M., Whittle, A.J., 1995. A compression model for cohesionless soils. Géotechnique 45 (4), 611–631.

Poorooshasb, H.B., 1989. Description of flow of sand using state parameters. Comput. Geotech. 8, 195–218.

Riemer, M.F., Seed, R.B., 1997. Factors affecting apparent position of steady-state line. ASCE J. Geotech. Geoenviron. Eng. 123 (3), 281–288.

Salgado, R., Bandini, P., Karim, A., 2000. Shear strength and stiffness of silty sand. J. Geotech. Geoenviron. Eng. 126 (5), 451–462.

Shipton, B., Coop, M.R., 2012. On the compression behaviour of reconstituted soils. Soils Found. 52 (4), 668–681.

Takahashi, A., Jardine, R.J., 2007. Assessment of standard research sand for laboratory testing. Q. J. Eng. Geol. Hydrogeol. 40 (1), 93–103.

Thevanayagam, S., Mohan, S., 2000. Intergranular state variables and stress–strain behaviour of silty sands. Géotechnique 50 (1), 1–23.

Verdugo, R., Ishihara, K., 1996. The steady state of sandy soils. Soils Found. 36 (2), 81–91.

Vilhar, G., Jovičić, V., Coop, M.R., 2013. The role of particle breakage in the mechanics of a non-plastic silty sand. Soils Found. 53 (1), 91–104.

Viggiani, G., Atkinson, J.H., 1995. Stiffness of fine-grained soil at very small strains. Géotechnique 45 (2), 249–265.

Wroth, C.P., Bassett, R.H., 1965. A stress–strain relationship for the shearing behaviour of a sand. Géotechnique 15 (1), 32–56.

Yamamuro, J.A., Lade, P.L., 1998. Steady-state concepts and static liquefaction of silty sands.. ASCE J. Geotech. Geoenviron. Eng., 124; 868–877.

Yang, Z.X., Li, X.S., Yang, J., 2008. Quantifying and modelling fabric anisotropy of granular soils. Géotechnique 58 (4), 237–248.

Zdravkovic, L., 1996. The Stress–Strain–Strength Anisotropy of a Granular Medium Under General Stress Conditions (Ph.D. Thesis).